THE JOURNAL OF PHYSICAL CHEMISTRY C

Article

pubs.acs.org/JPCC

A Combined Monte Carlo and Hückel Theory Simulation of Orientational Ordering in C_{60} Assemblies

Jeremy Leaf, Andrew Stannard, Samuel P. Jarvis, Philip Moriarty, and Janette L. Dunn*

School of Physics and Astronomy, University of Nottingham, Nottingham NG7 2RD, U.K.

Supporting Information

ABSTRACT: Orientational ordering of C_{60} molecules within monolayer and multilayer islands is a regularly observed phenomenon in scanning tunneling microscopy (STM) studies. Here we simulate the orientational ordering seen in STM images via a novel combination of Monte Carlo and Hückel theory methods and compare to experimental data. A measure of the repulsive interaction energy between two adjacent C_{60} molecules is precalculated by estimating and processing the electron density distribution between them. Many combinations of molecular orientations are considered to encompass all the details of the molecular orbitals. Precalculated intermolecular interaction energies are inputted into a simulated C_{60} island. Here, the center position of each molecule is fixed, but the molecules are allowed to rotate freely around their centers. A minimum in the total island free energy is sought by sequentially picking molecules at random and rotating them according to their neighbors. Results show significant correlation with experimentally observed features in both mono- and multilayered islands on a variety of different substrates.

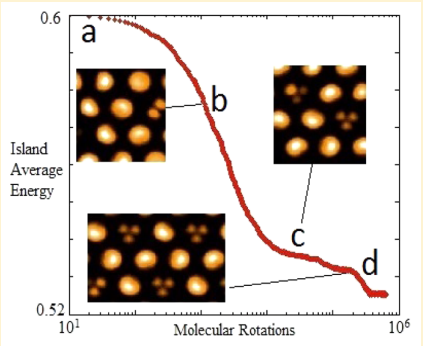

INTRODUCTION

When deposited onto substrates such as close-packed planes of fcc metals or NaCl multilayers, and given sufficient thermal energy, C_{60} molecules aggregate into islands. These islands assume a close-packed structure[1] for both monolayer and multilayer samples. At ambient temperature, molecules in multilayers will rotate freely around their centers.[2] Upon cooling below a transition temperature, free molecular rotations are frozen out.[2] In this state, C_{60} molecules reduce their respective interaction energies by rotating to a configuration whereby the total energy of the island is reduced.[3−10] In monolayers, the molecules will also rotate, but rotations are not free due to surface interactions. When imaged using scanning tunneling microscopy (STM), it is possible to distinguish between different molecular orientations by interpreting the shape of individual molecules.[11] Complex rotational order has been observed in both mono- and multilayered islands. Specific rotational structures typically depend on the substrate and on the layer thickness.[3−10]

In multilayered islands, and on a number of different substrates including NaCl, Au(111), and Cu(111), a variety of (2 × 2) "pinwheel" superstructures have been observed.[3,12] This is where a hexagon-down molecule, observed as a three-lobed feature in STM, is surrounded by double or single bond-down molecules, observed as two-lobed or single-lobed features, respectively, in a pinwheel formation. These (2 × 2) superstructures are often similar to those observed in bulk C_{60}.[2,13] An example of adsorption on NaCl is shown in Figure 1a.

On Cu(111), isolated C_{60} molecules are seen to sit with a hexagon face directed toward the surface (hexagon-down) and chemisorb on the surface. The hexagon face of the C_{60} will align with the (111) layer below. Two principal binding configurations at 180° to each other are available, as described by Larsson et al.[14] In an island, intermolecular interactions are sufficient to make one of the two configurations more favorable; the other is rarely seen, leading to the ordered (4 × 4) structure. Figure 1b shows an experimental STM image in which all except one molecule adopt the same most favorable configuration, with the remaining molecule adopting the least favorable orientation. Other molecular orientations are possible but are observed less frequently, such as pentagon-down molecules. On Au(111), the C_{60} molecules are less strongly bound than on Cu(111). This results in a higher proportion of pentagon-down molecules. In this paper we seek to understand why this variety of orientational orderings arises.

Most approaches to simulating C_{60} islands focus on monolayers. These typically involve fixing the molecules in a limited number of relative orientations and examining the system via density functional theory (DFT).[15−17] This, however, has the disadvantage that it is impossible to simulate a multilayer as the orientations of the molecules below are unknown. Moreover, only a few specific orientations are sampled. The dynamics of the molecular orientations are clearly a highly complex system due to the complexity of the observed

Received: January 20, 2016
Revised: March 30, 2016
Published: March 30, 2016

DOI: 10.1021/acs.jpcc.6b00638
J. Phys. Chem. C 2016, 120, 8139−8147

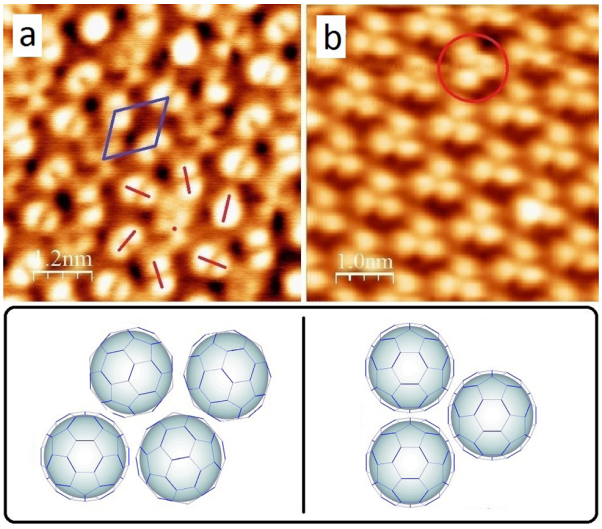

Figure 1. Two experimental STM images of C_{60} islands. Below are wire-frame representations of the molecular orientations. (a) A C_{60} multilayer on NaCl. An orientational "pinwheel" structure is observed where a hexagon-up molecule, indicated by a dot, is surrounded by six double-bond-up molecules, indicated by straight lines. The resultant (2 × 2) unit cell of the superstructure is indicated by a rhombus. These structures have previously been observed in other C_{60} layers.[3] (b) A commonly observed (4 × 4) superstructure on Cu(111), where C_{60} molecules in a monolayer all sit hexagon-up and align. Here one molecule has adopted the second, less favorable, orientation and is circled. Molecules in this hexagon-up configuration are also commonly seen on the Au(111) substrate.

rotational structures. Therefore, to gain a better understanding of the system, it is necessary to simulate very many more molecular configurations. A way to do this is via a Monte Carlo simulation. Unfortunately, it is impractical to use DFT to calculate the intermolecular interaction energies within a Monte Carlo study due to computing time limitations.

Laforge et al.[18] used a Monte Carlo simulation to model a bulk C_{60} system. A (2 × 2) pinwheel structure with molecular orientations similar to those seen in bulk C_{60} was generated. However, the size of their Monte Carlo simulation was only 2 × 2 molecules across, as shown by the unit cell in Figure 1, totaling only 12 molecules across 3 layers. This is not ideal due to edge effects and the inability to simulate nonuniform effects or defects. Significant differences in methodology described below have allowed us to simulate systems on a much larger scale, including monolayer and multilayer assemblies.

As the size of the simulated assembly increases, computation time increases dramatically. This is not only because there are more molecules to consider but also because increased degrees of freedom in the system lead to complex structures taking longer to appear in simulations. In Laforge et al.'s methodology,[18] intermolecular energies were calculated at every time step. This, however, limits the simulation size again due to computation time constraints. In this paper we demonstrate a methodology whereby a large number of intermolecular interactions are precalculated, leading to dramatic speed increases.

As there is no chemical bonding between the molecules in the C_{60} islands, we theorize that the molecules rotate to simply reduce the energy of the island due to intermolecular and surface interactions.[9] To simulate an island, we initially took two isolated molecules and examined the variation of the intermolecular energy. A unitless measure of the repulsive interaction energy was calculated for different molecular orientations via a novel application of the Hückel method. This process was completed for a high number of discrete relative orientations of the two molecules. Interactions with the surface substrate were also calculated. An island of molecules was then constructed. In this case, every molecule is allowed to rotate independently to an orientation chosen via a Monte Carlo simulation. We will show that the results of our model accurately reproduce the orientational order and defects observed experimentally.[3,6,19]

SIMULATION AND EXPERIMENTAL METHODS

Experimental Methods. We have investigated two key systems, C_{60}/Cu(111) and C_{60}/NaCl/Cu(111), as examples of systems with strong and weak molecule−substrate interactions, respectively. To acquire high quality images of C_{60} islands, we used a commercial (Createc) UHV, low-temperature STM/atomic force microscope (AFM) system. This provides images with submolecular resolution, which is a prerequisite for the analysis of the orientation of the adsorbed C_{60} molecules. The Cu(111) substrate was prepared via cycles of sputtering and annealing. C_{60} was also deposited onto a NaCl film prepared by depositing salt via a Knudsen cell onto a clean Cu(111) substrate (while the NaCl/Cu(111) sample was at room temperature). For both substrates, molecules were then deposited with the substrate cooled to 77 K. For isolated molecules to be observed on NaCl, the substrate was cooled to 4 K while depositing molecules. For imaging, the substrate was kept at either 4 or 77 K. At both of these temperatures, all molecular rotations are frozen out.

Simulation Methods. *Intermolecular and Surface Interactions.* In C_{60} islands and multilayers, molecular spacing is reduced at low temperature.[2,13] Below a threshold temperature, repulsive interactions will impede the molecules' free rotation and fix their orientations. Intermolecular repulsive interactions are primarily responsible for the resultant molecular orientations.[20] Here, attractive van der Waals forces provide a strong, but relatively uniform, field,[20] which means that their omission does not alter our overall results. Coulombic interactions, due to variations in charge density, have a similarly small effect on C_{60} molecular orientation,[20] and accurate predictions of rotational order have previously been obtained in Monte Carlo simulations excluding Coulombic interactions.[18] It should nevertheless be noted that this will not generally be true for other systems. Therefore, because our interest is solely in molecular rotation, only repulsive interactions will be considered.

Repulsive forces originate from a short-range Pauli exclusion regime, where overlapping orbitals from adjacent molecules distort at a very high energy cost. For this simulation, we choose not to use an analytical potential for intermolecular interactions. The commonly used Lennard-Jones potential ignores the complex orbital structure of the molecule. The potential developed by Lamoen and Michel[20] attempts to approximate the potential by placing repulsive Born−Mayer interaction centers along the bonds, but this is somewhat artificial. We therefore incorporate Hückel theory to model the true molecular orbital (MO) structure. Hückel theory models molecular orbitals via linear combination of atomic orbitals. It is ideally suited for molecules dominated by π bonding orbitals, such as C_{60}. As we only consider repulsive interactions, it makes

DOI: 10.1021/acs.jpcc.6b00638
J. Phys. Chem. C 2016, 120, 8139−8147

sense to limit the simulation to solely pairwise interactions. Thus, by considering two adjacent molecules and integrating over the multiplicative overlap of their molecular orbitals, we can extrapolate a repulsive interaction potential. Hückel theory does not directly calculate physical energies for MOs (estimated energies are returned as a function of an unknown β by solving the Schrödinger equation), but this is not a problem as the MO shapes are much more accurate. Because of its combined speed and accuracy, in terms of MO simulation, Hückel theory represents a powerful tool for the study of intermolecular interactions in C_{60} systems. We do not incorporate density functional theory (DFT) due to the extreme computation time cost involved. Hückel theory calculations are many orders of magnitude faster. However, a comparison of our model against van der Waals corrected DFT and a Lennard-Jones approach was performed for a selected set of relative molecular orientations (see Supporting Information). Our model correlates remarkably well with the Lennard-Jones results and demonstrates a qualitative match to the DFT results.

A significant surface interaction is also inherently present between C_{60} molecules and a Cu(111) or Au(111) substrate. To incorporate an interaction with these surfaces, we make it unfavorable for molecular orbitals to project into the surface. Atom-down and single-bond-down orientations then unfavorably project significant electron density into the surface, favoring the hexagon-down orientations observed experimentally. While this does not directly model the actual physics of the C_{60}−surface chemisorption, the resultant outputs are a good approximation to observed features. Using this model, the surface interaction has no influence on molecular rotations around the axis perpendicular to the substrate; only intermolecular interactions influence that degree of freedom.

Simulated STM Images and Intermolecular Interaction Calculation. Simulated STM images of isolated C_{60} molecules using the MOs from Hückel theory[21−23] accurately reproduce experimentally observed features, as shown in Figure 2 for molecules in three common orientations.

The MOs can also be used to estimate an interaction between two adjacent molecules. This is determined by integrating the multiplicative overlap of the two molecular orbitals, the area integrated being the bisecting plane between the two molecules. A grid of points is initially generated in the plane perpendicularly bisecting both molecules. The electron density from each molecule is then calculated at these grid points (Figure 3), taking account of all 30 filled states of each molecule. Note that if interactions with the surface split the Hückel molecular orbitals, the results will be unaffected as the set of filled orbitals remains the same.

The calculated planes of electron densities from each C_{60} are then multiplied together. In regions where there is a large overlap of the two electron densities, the multiplication returns large values for that region; conversely, in areas where there is little overlap, a set of small values is returned. The resultant grid is then summed to complete the integration and return the total interaction "energy" for that pair of molecules in that particular geometry, where

$$E = \sum_i \sum_j A(i, j)B(i, j) \tag{1}$$

A and B represent the grid of electron densities calculated from the molecule a and its adjacent molecule b, and i and j represent indices of the horizontal and vertical grid references, respectively.

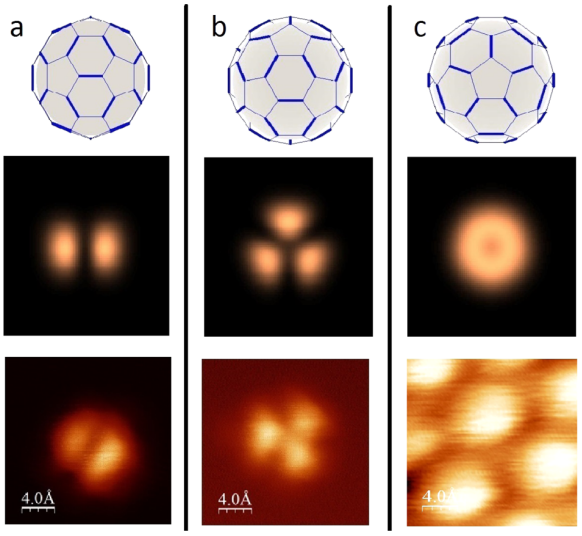

Figure 2. Three common molecular orientations as seen when looking down at the surface (top row). Their resultant simulated constant height STM scan (middle row). An experimental STM scan of a C_{60} molecule or molecules in that orientation (bottom row). (a) The LUMO of a C_{60} oriented double-bond-down. (b) The LUMO of a C_{60} oriented hexagon-down. (c) The LUMO of a C_{60} oriented pentagon-down. In (a) and (b) the experimental images show isolated C_{60} molecules pinned to an NaCl step edge, imaged at in constant-height STM at 4 K. (c) shows a monolayer cluster of pentagon-down C_{60} molecules on Cu(111). Images by STM at 77 K. Note that if a hexagon/pentagon/double-bond, etc., faces the surface, a hexagon/pentagon/double-bond, etc., will also be facing up away from the surface due to the icosahedral symmetry of the C_{60} molecule.

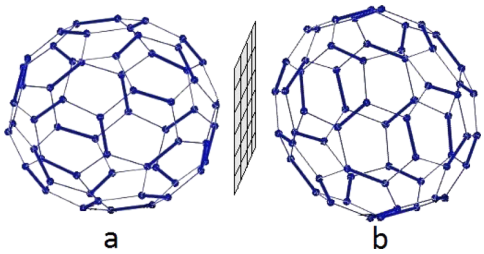

Figure 3. Grid between molecules a and b shows the locations where the electron density interactions are calculated.

The surface interaction was calculated by taking a grid directly below the molecule. This was then squared and summed to give

$$E_{SI} = \sum_i \sum_j A(i, j)^2 \tag{2}$$

which makes any orbitals projecting into the surface "high energy" configurations. The exact form of this surface interaction is not highly important; other similar forms that penalize projecting orbitals produce very similar results. The two molecules are then rotated to a second set of orientations, and the energies between them are recalculated. This process is repeated until all significant relative orientations between the two molecules have had an energy calculated and stored in a table. The angular increment between orientations was set to approximately 3° so as to capture all orientations of interest and

DOI: 10.1021/acs.jpcc.6b00638
J. Phys. Chem. C 2016, 120, 8139−8147

get good resolution of intermediate orientations. The energy values for the surface interaction and the intermolecular interaction were normalized, resulting in a table of energies ranging from 0 to 1. This negates the adverse effect of the resolution of the grid affecting the magnitude of the resultant energy spectrum.

A major issue for this method is the physical size of the table, in terms of both its initial calculation and its subsequent storage. If all possible molecular orientational configurations for the molecule and each of its 12 neighbors (in a multilayer) were to be considered, the lookup table would have approximately 1×10^{12} elements. This would be impossible to hold in the memory of a computer and would take months to calculate. It is therefore necessary to consider the symmetry of the molecule to cut down on the number of possible orientations that need to be calculated.

A molecular orientation can be defined with two components: first, a point on the surface of the molecule from where the molecule is observed; second, a rotation around an axis passing through that point and the center of the molecule. Figure 4 shows the smallest "unit cell" of the

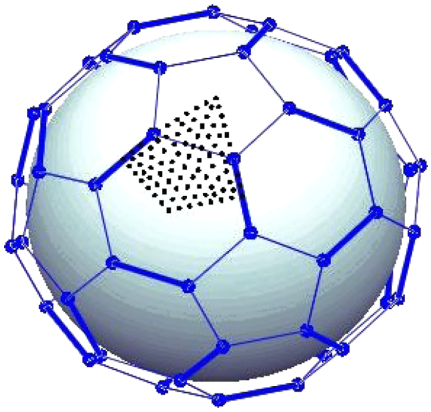

Figure 4. A net of points is superimposed on a C_{60} molecule. These define points on axes through the molecular center, from which molecular orientations can be defined. The area covered by these points represents the smallest possible area to capture all the information about the intermolecular interactions.

molecule that contains all of the points that must be calculated. The mesh of points was generated such that the points were evenly spaced across the unit cell. The number of molecular orientations available to the simulation is thus the number of points multiplied by the number of rotation segments to rotate about that point. In our simulation 94 points and 90 rotation segments leads to 8460 unique molecular orientations.

For every unique molecular orientation, 14 vectors are generated that point toward adjacent molecules and features of interest, as seen in Figure 5. For each surrounding vector, a perpendicular grid of coordinates is calculated and the molecular electron density calculated at each grid coordinate. This is the only time the electron density needs to be calculated, which contributes to the overall speed of the procedure.

These grids of electron density are then used in eq 1 according to their relative positions. That is to say, for a single orientation of the center molecule, it will compare its 12 grids (via eq 1) with its neighbor's grids pointing toward itself. As an example, consider the comparison of a molecule with its top

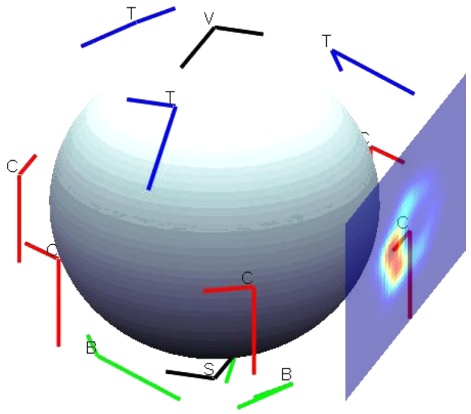

Figure 5. This image represents 14 surrounding vectors (generated from a single unique molecular orientation) from which electron density grids are calculated. Each L-shaped line represents three components necessary to generate the grid at which the electron density is calculated. These are (i) the distance between the center of the molecule and the L defining the distance from the molecule the grid is calculated, (ii) the long arm of the L pointing toward the bottom of the grid, and (iii) the short arm pointing toward the right side of the grid. It is critical that the grid orientations and locations are correctly defined. If not, they will not line up with the grid for an adjacent molecule. Lines labeled C point toward the six adjacent molecules in the same layer as the current C_{60}. The lines labeled B and T point toward molecules in the bottom and top layer around the molecule, respectively. The line labeled S directly below the molecule points toward the surface to calculate the surface interaction. Finally, the line labeled V above the molecule points up from the island and is used to generate an image so the viewer can know what orientation the molecule is in. A grid of points directed toward an adjacent molecule and the respective calculated electron density is shown to illustrate its position/orientation.

right neighbor in the same molecular layer. The molecule would submit its top-right grid points as defined by its current orientation, and its neighbor would submit its bottom-left grid point as defined by its molecular orientation. For every unique molecular orientation of the center molecule *a*, the adjacent molecule must be rotated and compared for all of its molecular orientations. This must be completed for all 12 neighbors.

Finally, the grid for the adjacent molecule *b* must be flipped horizontally before being compared to the grid from molecule *a*, as a grid observed from an adjacent molecule will have its *i* coordinates reversed. This can be seen in Figure 5 where two opposite points, labeled C, will have their horizontal components reversed.

This procedure returns an energy lookup table for every molecular orientation on every side of the molecule and every adjacent molecular orientation. For 8460 unique molecular orientations and considering the 12 adjacent molecules, there are $\approx 10^9$ unique intermolecular interactions that must be calculated. The table generation was single-threaded and written in MATLAB. It took only 6 h to generate on a desktop computer using a single 3.2 GHz processor core and 12 GB of RAM. A large (60 GB on an SSD) page file was used during the table generation which significantly slowed down the procedure. The final intermolecular interaction table was 7 GB, which easily fits in RAM.

Monte Carlo Simulations. A kinetic Monte Carlo simulation was written to consider a cubic island of hexagonally packed C_{60} molecules with periodic boundary conditions (Figure 6). A

DOI: 10.1021/acs.jpcc.6b00638
J. Phys. Chem. C 2016, 120, 8139−8147

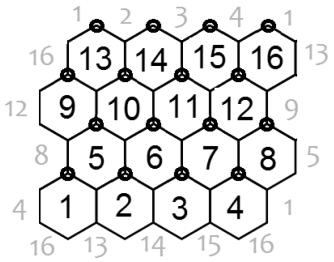

Figure 6. A 4 × 4 island is shown with corresponding periodic boundary neighbors labeled. The small circles represent the location of molecules in the case of a second layer above. A third layer has the same relation to the second layer as the second has to the first.

molecule is chosen at random and rotated to a new orientation. All precalculated orientations are available for molecular rotation, where the probability of a molecule attaining a particular orientation is weighted according to its energy landscape. Additionally, the molecules center positions are fixed. This is an approximation as molecules could undergo small local shifts in position as a result of orientational order, and surface vacancy formation could additionally lead small changes in molecular height, but these changes are likely to be small. The island must have an even side length but can otherwise be arbitrarily scaled up in size. For multilayers, an FCC, or "ABC" packing arrangement is employed. The starting state of the island is with all molecules orientated randomly. The Monte Carlo algorithm uses the energy landscape for a molecule defined by the orientations of its surrounding molecules and a surface interaction. This landscape is a table of all the possible orientations the molecule could take and the energy it would be at if it took that orientation. The energy E_i, for each molecular configuration i, is calculated by summing all the pairwise interactions with adjacent molecules and a surface interaction, E_{SI}. A constant, α, is used to vary the strength of the surface interaction relative to the intermolecular interactions. As the surface interaction is artificial in form, it is necessary to manually calibrate it against intermolecular interactions. A low value of α means intermolecular interactions dominate the simulation dynamics, whereas a high value reverses this.

A simple kinetic Monte Carlo algorithm is then implemented to choose the next orientation for the molecule. The C_{60} island is considered as a canonical ensemble, using a Boltzmann distribution to model the final state probability, so that

$$P_i = Z^{-1} \exp\left(\frac{-E_i}{T}\right) \tag{3}$$

Here P_i is the probability of the molecule taking the ith orientation, E_i is the energy of that orientation, T is the temperature in energy units, and Z is defined as

$$Z = \sum_i \exp\left(\frac{-E_i}{T}\right) \tag{4}$$

Because of the method of its calculation, the magnitude of E_i is arbitrary. The value is dimensionless—a relative energy that is self-consistent. Thus, the temperature T is set at an arbitrary magnitude to display the dynamics of the system. Once a new molecular orientation for the molecule has been chosen, it is rotated to that orientation, a new molecule is randomly chosen, and the process is repeated. As the simulation progresses, the average energy of the island will fall until it equilibrates.

Simulation Metrics and Parameters. A number of simulation metrics and parameters can be observed and set to control and observe the ordering in the island.

As E_i is generated using Hückel theory, the actual value for the interaction energy is not known. Thus, the temperature T is set at an arbitrary magnitude to display the dynamics of the system. As such, no Boltzmann constant is included in eqs 3 and 4 as its inclusion would still not result in T representing the real temperature of the system. This is to say, a low temperature is set such that a molecule will almost certainly go to its lowest energy state. A medium temperature is such that a molecule has a range of discrete orientations available that it could move to. A high temperature is seen as the molecules having no bias toward any particular orientation. This is shown in Figure 7.

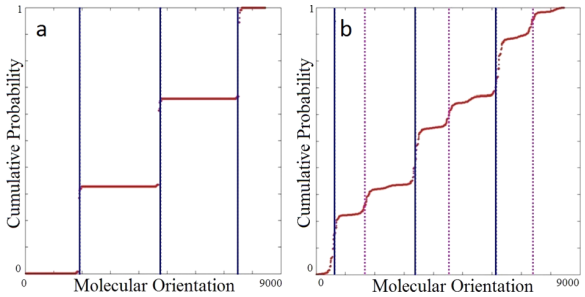

Figure 7. Cumulative probability distribution for a single molecule generated from the energy landscape it experiences. Its energy landscape is defined by its surrounding molecules. The x-axis relates to all 8460 unique orientations the molecule can hold. (a) At low temperatures, three orientations are likely relating to three equivalent 120° rotations around a hexagon-down configuration in a C_{60}/Cu(111) island. These orientations are highlighted by the vertical lines in the figure. (b) At high temperatures other orientations become more likely and can be seen as additional features in the graph. Here a molecule sits at the interface between two phases of hexagon-down C_{60} molecules. Each phase contains molecules in one of the preferential binding orientations for C_{60} on Cu(111) (at 180° from each other). This can be seen in (b) as it is favorable for the molecule to be in either 3-fold symmetry orientation designated by the solid and dashed lines.

Island equilibrium is defined by the island energy minimizing and remaining static for a period of time equivalent to 10× the timesteps taken to reach that minimum. The average energy of the island is defined as the sum of all the intermolecular and surface interaction energies, divided by the total number of intermolecular interactions and surface interactions.

The Shannon entropy

$$S = -\sum_i n_i \log_2(n_i) \tag{5}$$

where n_i is the fraction of molecules in a particular orientation i, is used as a measure of the number of molecules in different orientations.

Even though the lookup table is 7 GB, the simulation only needs to process small segments of it at a time and so the speed at which the energy equilibrates is very fast. When considering a monolayer of 100 molecules, the system will equilibrate in a simulation time of under 15 s on a desktop PC.

DOI: 10.1021/acs.jpcc.6b00638
J. Phys. Chem. C 2016, 120, 8139−8147

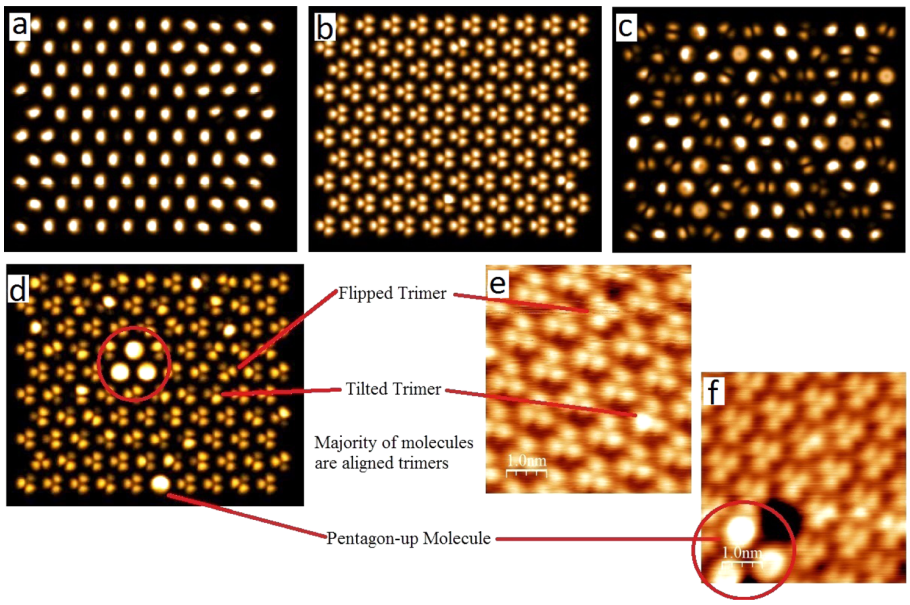

Figure 8. A series of 10 × 10 monolayer simulations. (a) No surface interaction has been included here, and the molecules are aligned single bond up. (b–d) Varying simulation temperature with a strong Cu(111) surface interaction included, where (b) is a low temperature simulation where all molecules align perfectly. (c) A high temperature simulation showing a fully disordered layer. (d, e, f) A mid-temperature simulation is compared to two experimental STM images and similar features identified. An experimental and simulated cluster of pentagon-down molecules are circled in (d) and (f). STM images taken at 4 K.

RESULTS

Monolayer Simulations. Simulations were initially targeted at monolayer islands. The intermolecular separation (center to center) was set at 1.02 nm to match experimental images. However, it was noted that modifying this distance did not affect simulation outcomes. In addition, due to the speed at which monolayers equilibrated, a large 10 × 10 simulation size was selected. When no surface interaction is included, the resultant molecules align single bond up, with hexagons aligning toward surrounding molecules. This is not realistic behavior for adsorption on Cu(111) or Au(111) and thus shows that the surface interaction needs to be included (Figure 8a). When a surface interaction is included as discussed previously, the resulting simulated order correlates well with STM data for both Cu(111) and Au(111). This confirms that the observed hexagon-prone orientation of the molecules is driven by the substrate bonding and shows that intermolecular interactions assist in determining orientation with respect to rotation around an axis perpendicular to the substrate.

Cu(111) Monolayers. By including a strong surface interaction, we simulate a Cu(111) substrate. The simulated islands display many features observed in STM images of actual islands. Similar features are compared in Figure 8 and include a broad ordered structure (aligned hexagon-down molecules—seen as trimers), isolated or clustered pentagon-down molecules (seen as disk-shaped molecules), flipped hexagon-down molecules that are reversed to the normal orientation, and finally tilted hexagons/pentagons which can be seen as molecules where one side is notably brighter than the other.

It is important to note in Figure 8 that for medium temperatures a molecule observed in a pentagon-down or flipped-trimer configuration is in a local minimum as seen in Figure 7b. This means that the next time the molecule is considered by the Monte Carlo algorithm, it may move to a different energy minimum. Experimentally, pentagon-down and tilted pentagon-down molecules are rarely seen. When they are observed, they will either be isolated or form small clusters, as seen by the three pentagon-down molecules in Figures 8f and 2c. This clustering of pentagon-down and tilted pentagon-down molecules is routinely seen in simulation whereby these molecular orientations are observed as more stable when clustered (Figure 8d). For a mid-level temperature simulation, these pentagon-down molecules, etc., fluctuate around the surface. These time-dependent fluctuations are not observed in the STM images as they show molecules that have been rapidly cooled and had these fluctuations frozen in.

Au(111) Monolayers. C_{60} molecules are not so strongly bound to an Au(111) substrate as compared to a Cu(111) substrate. This typically manifests as a higher proportion of molecules showing a pentagon-up, or similar nonuniform, orientation. It is easier for the molecules to rotate away from the low-energy, hexagon-up, orientation. The resultant surface can be a disordered $(2\sqrt{3}\times 2\sqrt{3})R30^\circ$ superstructure. A characteristic of C_{60}/Au(111) substrates involves the boundary between two domains of hexagon-up molecules, each domain in one of the two C_{60} principal binding configurations. Here the two domains are separated by a boundary of pentagon-up molecules.[10,19] In simulation, by reducing the surface interaction compared to Cu(111), pentagon-up molecules are more commonly seen. As observed in experiment, the interface between two domains of C_{60} molecules is populated by tilted pentagon-up molecules (Figure 9). Initially, in simulation, most molecules adopt a tilted pentagon-up orientation. Then, as the energy minimizes, domains of hexagon-up molecules start to nucleate, grow, and merge. As the simulation progresses, one of the domains will dominate. The other domain, surrounded by a barrier of pentagon-up molecules, will slowly be eroded and eventually disappear. It was also noted that pentagon-down defects were far more common in higher simulation temperatures. The simulation has displayed excellent agreement with

DOI: 10.1021/acs.jpcc.6b00638
J. Phys. Chem. C 2016, 120, 8139–8147

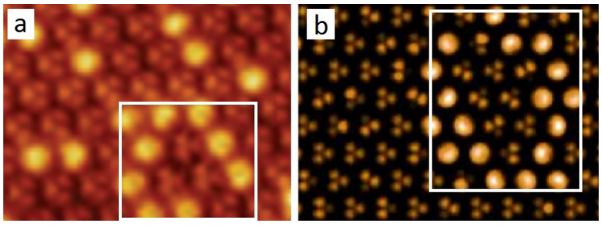

Figure 9. (a) An STM image of a C_{60} monolayer on Au(111). Reproduced with permission from ref 19. Copyright 2011 AIP Publishing LLC. Circled is a cluster of molecules in the second principal binding configuration, surrounded by a wall of pentagon-up molecules. (b) A simulation with a reduced surface interaction showing two phases of C_{60} molecules and the boundary layer between them.

monolayer C_{60} islands on multiple substrates. Different temperature levels mirror what is observed in actual STM images.

Multilayer Simulations. The simulation size for multilayers was kept at 8 × 8, which was considered to be a reasonable size to mitigate edge effects while keeping simulation time down. In an 8 × 8 simulation a central molecule will have either 3 or 4 molecules between it and an edge.

A multilayered simulation will not minimize its energy as easily as a monolayer due to the energy landscape being significantly more complex. As a multilayer simulation progresses, the molecules will go through a number of intermediate phases or reconstructions before equilibrating (Figure 10). These can act as local minima which the

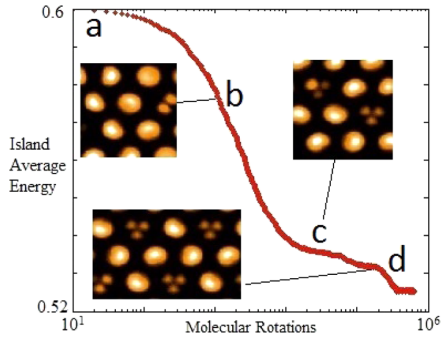

Figure 10. Average island energy as a function of the number of molecular rotations (i.e., time). (a) The starting, high-energy configuration. Molecular orientations are random at the start of the simulation. (b) Molecules quickly align themselves approximately pentagon-down, single-bond-down, and atom-down. (c) Different (2 × 2) domains form; these are separated by antiphase boundaries and "compete" in terms of the expansion of a given phase. (d) One (2 × 2) domain dominates. Once a sufficient number of molecules are in that domain, a critical point is reached which triggers the conversion of all molecules to that (2 × 2) domain.

simulation can get trapped in. Because local minima are often long-range structures within the island, it can be difficult for the Monte Carlo algorithm to escape them. This is because only one molecule is considered at a time; its surrounding energy landscape remains static, and so the local minima structure would remain. In real islands, all the molecules rotate simultaneously until a minimum is reached. Nevertheless, (2 × 2) superstructures have been simulated that closely resemble the C_{60} rotational reconstructions observed by Rossel et al.[3] where a bilayer of C_{60} molecules on NaCl exhibited rotational order (Figure 11). Here no surface interaction is included due

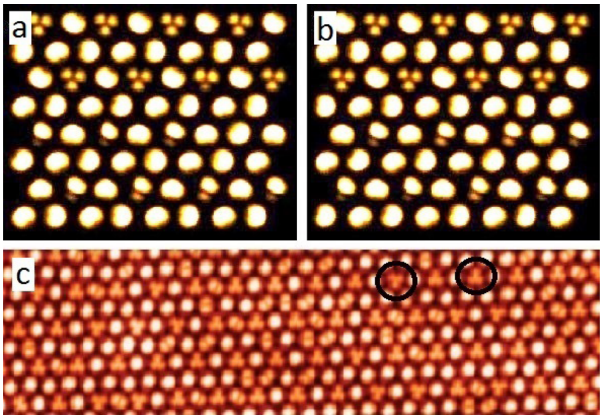

Figure 11. A bilayer island simulation with an intermolecular separation of 1.05 nm, where (a) is the bottom and (b) top layer in the island. The bottom layer (a) has no surface interaction included. In (a) and (b) the top half of the simulation is similar to (c), whereby hexagon-up molecules are surrounded by tilted pentagon-up molecules. The bottom half demonstrates a nonphysical local minima that the simulation has been trapped in. (c) STM image of bilayer C_{60} on NaCl/Au(111). Reprinted with permission from ref 3. Copyright 2011 American Physical Society. Intermolecular separation is measured at 1.05 ± 0.05 nm. A (2 × 2) superstructure has developed which is similar to that seen in (a, b). Note circled C_{60} molecules are oriented 180° to each other. This behavior can sometimes be observed in simulation while it is minimizing in energy.

to molecular decoupling at the C_{60}/NaCl interface.[24,25] Experimentally and in simulation, there are dissimilarities to the more common (2 × 2) configuration observed in Figure 1a and bulk C_{60}. Here, double-bond-up molecules are replaced by tilted pentagon-up molecules.

A quad layer has also been simulated atop a Cu(111) substrate. This has demonstrated how a (2 × 2) superstructure similar to bulk C_{60} can develop from a layer of molecules that are influenced by a surface interaction. If intermolecular interactions between the bottom layer and second layer in the island are left as normal, the molecules in the bottom layer will reconstruct to a (2 × 2) superstructure. Here all the molecules remain hexagon-prone due to the surface interaction, but 1/4 molecules have a 60° rotation around an axis perpendicular to the surface. In this case the bulk-like reconstruction will develop immediately from the second layer upward. Because of the binding configurations of C_{60} on Cu(111), however, this might not be physical. Thus, the interaction of the second layer affecting the bottom layer is reduced so as to maintain the (1 × 1) structure seen in monolayers. This is the case seen in Figure 12. Here a bulk-like reconstruction was achieved in simulation via a boundary layer between bottom layer (hexagon-down (1× 1) reconstruction) and third layer ((2 × 2) reconstruction). This boundary layer exhibits a tilted double bond (or atom-down) configuration in a (2 × 1) superstructure.

It was noted that the (2 × 2) structure shown in Figure 12c,d develops much more readily if the island is three or more layers thick. For the structure to develop, it will initially nucleate in the central layers and then spread throughout the rest of the

DOI: 10.1021/acs.jpcc.6b00638
J. Phys. Chem. C 2016, 120, 8139−8147

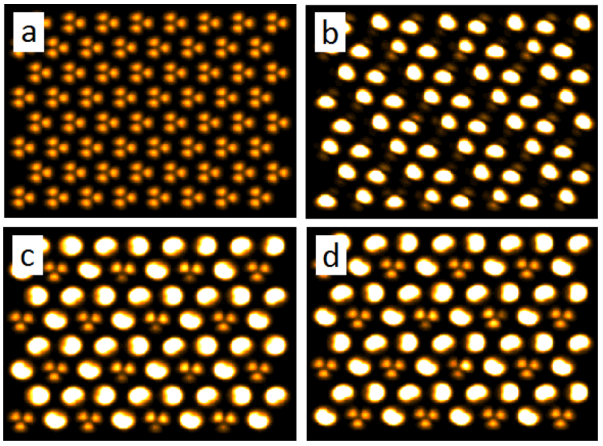

Figure 12. A four-layer island where (a)−(d) represent the lowest to highest layers, respectively. The first layer (a) has a surface interaction included and a reduced interaction with the layer above to simulate a Cu(111) substrate. By the third layer (c), a (2 × 2) superstructure has developed. An intermediate reconstruction has developed in (b) to bridge the rigid (1 × 1) structure forced by the surface and the more favorable (2 × 2) phase. The intermediate reconstruction exhibits tilted double-bond-prone molecules.

island. Thus, this structure will only occasionally appear in simulated bilayer islands but will almost always appear in three or more layered islands. Additionally, the (2 × 2) structure is observed to be more stable in the central layers. Layers that have a surface exposed are less stable, especially hexagon-down molecules. This corroborates experimental results where surface molecular rotational disorder is enhanced on the surface molecular layer.[26] Additionally, this supports Laforge et al.'s prediction that the surface hexagon-down molecule is in a shallower energy well than the other three molecules in the unit cell. A video of a monolayer and multilayer simulation is included in the Supporting Information.

CONCLUSIONS

A large-scale Monte Carlo simulation of orientational ordering in C_{60} assemblies has been developed, which incorporated a number of new computational approaches. These included a novel use of the Hückel method to calculate an intermolecular repulsive term, in addition to utilizing the C_{60} molecular symmetry to reduce computation time. Using these tools, a lookup table of pairwise intermolecular interactions was generated for a high number of relative molecular orientations. Additionally, a surface interaction was included to mimic a Cu(111)/C_{60} and Au(111)/C_{60} interaction.

Our simulation strategy has successfully reproduced observed structures in mono- and multilayered C_{60} islands. These simulations have been facilitated by an extremely fast computation time. Cu(111)/monolayer C_{60} simulations show good agreement with experiment, including defects and clusters of pentagon-down molecules. In multilayers, (2 × 2) structures have been reproduced similar to ones observed in a C_{60} bilayer on NaCl.[3] Additionally, with a surface interaction present, (2× 2) structures have been observed developing in upper layers of a simulated island. These were facilitated by a boundary layer of molecules.

Further work could attempt to calibrate the simulation to physical temperatures and modify the intermolecular interaction to incorporate sp^2 orbitals or attractive van der Waals forces. The periodic boundary conditions could also be removed to model irregularly shaped islands or island growth. In addition, single molecules could be removed from the simulation to see if vacancies have an effect on rotational structure.

ASSOCIATED CONTENT

Supporting Information

The Supporting Information is available free of charge on the ACS Publications website at DOI: 10.1021/acs.jpcc.6b00638.

A video of two Monte Carlo simulations: one is a monolayer of C_{60} molecules on a Cu(111) substrate, and one is a multilayer on an NaCl/Cu(111) substrate (note especially the fine detail of molecular movement and phase separations during energy minimizations) (AVI)

A figure showing a comparison between our Hückel-based intermolecular potential, a Lennard-Jones potential, and a DFT calculation (PDF)

AUTHOR INFORMATION

Corresponding Author

*E-mail janette.dunn@nottingham.ac.uk (J.L.D.).

Notes

The authors declare no competing financial interest.

ACKNOWLEDGMENTS

The authors thank Dr. Andrew J. Lakin for his valuable conversations and input. S.P.J. thanks the Leverhulme Trust for the award of fellowship ECF-2015-005. J.M.L. acknowledges funding from the EPSRC through the doctoral training grant EP/L50502X/1.

REFERENCES

(1) Murray, P. W.; Pedersen, M. O.; Lægsgaard, E.; Stensgaard, I.; Besenbacher, F. Growth of C_{60} on Cu (110) and Ni (110) surfaces: C_{60}-induced interfacial roughening. *Phys. Rev. B: Condens. Matter Mater. Phys.* **1997**, *55*, 9360−9363.

(2) David, W. I. F.; Ibberson, R. M.; Dennis, T. J. S.; Hare, J. P.; Prassides, K. Structural phase transitions in the fullerene C_{60}. *Europhys. Lett.* **1992**, *18*, 219−225.

(3) Rossel, F.; Pivetta, M.; Patthey, F.; Ćavar, E.; Seitsonen, A. P.; Schneider, W.-D. Growth and characterization of fullerene nanocrystals on NaCl/Au (111). *Phys. Rev. B: Condens. Matter Mater. Phys.* **2011**, *84*, 075426.

(4) Schull, G.; Berndt, R. Orientationally ordered (7× 7) superstructure of C_{60} on Au (111). *Phys. Rev. Lett.* **2007**, *99*, 226105.

(5) Liu, C. D.; Qin, Z. H.; Chen, J. A.; Guo, Q. M.; Yu, Y. H.; Cao, G. Y. Molecular orientations and interfacial structure of C_{60} on Pt (111). *J. Chem. Phys.* **2011**, *134*, 044707.

(6) Hashizume, T.; Motai, K.; Wang, X. D.; Shinohara, H.; Saito, Y.; Maruyama, Y.; Ohno, K.; Kawazoe, Y.; Nishina, Y.; Pickering, H. W.; Kuk, Y.; Sakurai, T. Intramolecular structures of C_{60} molecules adsorbed on the Cu (111)-(1× 1) surface. *Phys. Rev. Lett.* **1993**, *71*, 2959−2962.

(7) Bozhko, S. I.; Taupin, V.; Lebyodkin, M.; Fressengeas, C.; Levchenko, E. A.; Radikan, K.; Lübben, O.; Semenov, V. N.; Shvets, I. V. Disclinations in C_{60} molecular layers on WO_2/W(110) surfaces. *Phys. Rev. B: Condens. Matter Mater. Phys.* **2014**, *90*, 214106.

(8) Paßens, M.; Waser, R.; Karthäuser, S. Enhanced fullerene-Au (111) coupling in $(2\sqrt{3}\times 2\sqrt{3})R30°$ superstructures with intermolecular interactions. *Beilstein J. Nanotechnol.* **2015**, *6*, 1421−1431.

(9) Yuan, L.-F.; Yang, J.; Wang, H. Q.; Zeng, C. G.; Li, Q. X.; Wang, B.; Hou, J. G.; Zhu, Q. S.; Chen, D. M. Low-temperature orientationally ordered structures of two-dimensional C_{60}. *J. Am. Chem. Soc.* **2003**, *125*, 169−172.

DOI: 10.1021/acs.jpcc.6b00638
J. Phys. Chem. C 2016, 120, 8139−8147

(10) Paßens, M.; Karthäuser, S. Interfacial and intermolecular interactions determining the rotational orientation of C_{60} adsorbed on Au (111). *Surf. Sci.* **2015**, *642*, 11−15.
(11) Hou, J. G.; Yang, J.; Wang, H.; Li, Q.; Zeng, C.; Lin, H.; Bing, W.; Chen, D. M.; Zhu, Q. Identifying molecular orientation of individual C_{60} on a Si (111)-(7× 7) surface. *Phys. Rev. Lett.* **1999**, *83*, 3001−3004.
(12) Wang, H.; Zeng, C.; Wang, B.; Hou, J. G.; Li, Q.; Yang, J. Orientational configurations of the C_{60} molecules in the (2× 2) superlattice on a solid C_{60} (111) surface at low temperature. *Phys. Rev. B: Condens. Matter Mater. Phys.* **2001**, *63*, 085417.
(13) Heiney, P. A.; Fischer, J. E.; McGhie, A. R.; Romanow, W. J.; Denenstein, A. M.; McCauley, J. P., Jr.; Smith, A. B.; Cox, D. E. Orientational ordering transition in solid C_{60}. *Phys. Rev. Lett.* **1991**, *66*, 2911−2914.
(14) Larsson, J. A.; Elliott, S. D.; Greer, J. C.; Repp, J.; Meyer, G.; Allenspach, R. Orientation of individual C_{60} molecules adsorbed on Cu (111): low-temperature scanning tunneling microscopy and density functional calculations. *Phys. Rev. B: Condens. Matter Mater. Phys.* **2008**, *77*, 115434.
(15) Casarin, M.; Forrer, D.; Orzali, T.; Petukhov, M.; Sambi, M.; Tondello, E.; Vittadini, A. Strong bonding of single C_{60} molecules to (1× 2)-Pt (110): an STM/DFT investigation. *J. Phys. Chem. C* **2007**, *111*, 9365−9373.
(16) Krasnikov, S. A.; Bozhko, S. I.; Radican, K.; Lübben, O.; Murphy, B. E.; Vadapoo, S.-R.; Wu, H.-C.; Abid, M.; Semenov, V. N.; Shvets, I. V. Self-assembly and ordering of C_{60} on the WO_2/W(110) surface. *Nano Res.* **2011**, *4*, 194−203.
(17) Wang, L.-L.; Cheng, H.-P. Density functional study of the adsorption of a C_{60} monolayer on Ag (111) and Au (111) surfaces. *Phys. Rev. B: Condens. Matter Mater. Phys.* **2004**, *69*, 165417.
(18) Laforge, C.; Passerone, D.; Harris, A. B.; Lambin, P.; Tosatti, E. Two-stage rotational disordering of a molecular crystal surface: C_{60}. *Phys. Rev. Lett.* **2001**, *87*, 085503.
(19) Tang, L.; Xie, Y. C.; Guo, Q. M. Complex orientational ordering of C_{60} molecules on Au (111). *J. Chem. Phys.* **2011**, *135*, 114702.
(20) Lamoen, D.; Michel, K. H. Crystal field, orientational order, and lattice contraction in solid C_{60}. *J. Chem. Phys.* **1994**, *101*, 1435−1443.
(21) Hands, I. D.; Dunn, J. L.; Bates, C. A. Calculation of images of oriented C_{60} molecules using molecular orbital theory. *Phys. Rev. B: Condens. Matter Mater. Phys.* **2010**, *81*, 205440.
(22) Lakin, A. J.; Chiutu, C.; Sweetman, A. M.; Moriarty, P.; Dunn, J. L. Recovering molecular orientation from convoluted orbitals. *Phys. Rev. B: Condens. Matter Mater. Phys.* **2013**, *88*, 035447.
(23) Chiutu, C.; Sweetman, A. M.; Lakin, A. J.; Stannard, A.; Jarvis, S.; Kantorovich, L.; Dunn, J. L.; Moriarty, P. Precise orientation of a single C_{60} molecule on the tip of a scanning probe microscope. *Phys. Rev. Lett.* **2012**, *108*, 268302.
(24) Cañas-Ventura, M. E.; Xiao, W.; Ruffieux, P.; Rieger, R.; Müllen, K.; Brune, H.; Fasel, R. Stabilization of bimolecular islands on ultrathin NaCl films by a vicinal substrate. *Surf. Sci.* **2009**, *603*, 2294−2299.
(25) Pfeiffer, O.; Gnecco, E.; Zimmerli, L.; Maier, S.; Meyer, E.; Nony, L.; Bennewitz, R.; Diederich, F.; Fang, H.; Bonifazi, D. Force microscopy on insulators: imaging of organic molecules. *J. Phys.: Conf. Ser.* **2005**, *19*, 166−174.
(26) Goldoni, A.; Cepek, C.; Modesti, S. First-order orientational-disordering transition on the (111) surface of C_{60}. *Phys. Rev. B: Condens. Matter Mater. Phys.* **1996**, *54*, 2890−2895.

DOI: 10.1021/acs.jpcc.6b00638
J. Phys. Chem. C 2016, 120, 8139−8147